THE JOURNAL OF BIOLOGICAL CHEMISTRY VOL. 284, NO. 8, pp. 4952–4959, February 20, 2009
Printed in the U.S.A.

Deoxygenated Disaccharide Analogs as Specific Inhibitors of β1–4-Galactosyltransferase 1 and Selectin-mediated Tumor Metastasis*[S]

Received for publication, July 28, 2008, and in revised form, December 3, 2008 Published, JBC Papers in Press, December 23, 2008, DOI 10.1074/jbc.M805782200

Jillian R. Brown[‡1], Feng Yang[‡], Anjana Sinha[‡], Boopathy Ramakrishnan[§¶], Yitzhak Tor[‖], Pradman K. Qasba[§], and Jeffrey D. Esko[‡2]

From the [‡]Department of Cellular and Molecular Medicine, Glycobiology Research and Training Center, and the [‖]Department of Chemistry and Biochemistry, University of California, San Diego, La Jolla, California 92093 and the [§]Structural Glycobiology Section, Nanobiology Program, and [¶]Basic Research Program SAIC-Frederick Inc., Center for Cancer Research, NCI-Frederick, National Institutes of Health, Frederick, Maryland 21702

The disaccharide peracetylated GlcNAcβ1–3Galβ-*O*-naphthalenemethanol (disaccharide 1) diminishes the formation of the glycan sialyl Lewis X (Neu5Acα2–3Galβ1–4(Fucα1–3)GlcNAc; sLe^X) in tumor cells. Previous studies showed that the mechanism of action of disaccharide 1 involves three steps: (i) deacetylation by carboxyesterases, (ii) action as a biosynthetic intermediate for downstream enzymes involved in sLe^X assembly, and (iii) generation of several glycans related to sLe^X. In this report, we show that GlcNAcβ1–3Galβ-*O*-naphthalenemethanol binds to the acceptor site of human β1–4-galactosyltransferase much like the acceptor trisaccharide, GlcNAcβ1–2Manβ1–6Man, which is present on *N*-linked glycans. The 4′-deoxy analog, in which the acceptor hydroxyl group was replaced by -H, did not act as a substrate but instead acted as a competitive inhibitor of the enzyme. The acetylated form of this compound inhibited sLe^X formation in U937 monocytic leukemia cells, suggesting that it had inhibitory activity *in vivo* as well. A series of synthetic acetylated analogs of 1 containing -H, -F, $-N_3$, $-NH_2$, or $-OCH_3$ instead of the hydroxyl groups at C-3′- and C-4′-positions of the terminal *N*-acetylglucosamine residue also blocked sLe^X formation in cells. The reduction of sLe^X by the 4′-deoxy analog also diminished experimental tumor metastasis by Lewis lung carcinoma *in vivo*. These data suggest that non-substrate disaccharides have therapeutic potential through their ability to bind to glycosyltransferases *in vivo* and to alter glycan-dependent pathologic processes.

The sialylated, fucosylated tetrasaccharide, sLe^X,[3] is a common carbohydrate determinant present in many *O*-GalNAc-linked mucins and *N*-linked glycans that act as selectin ligands (see Ref. 1 and references therein). Expression of sLe^X endows tumor cells with the capacity to bind to platelets and endothelial cells in the vasculature via P- and E-selectins, thus facilitating hematogenous metastasis possibly through protection against innate immune cells and by adhesion to the blood vessel wall. Strategies for blocking selectin-carbohydrate interactions include (i) competition by soluble recombinant forms of selectins, glycoprotein ligands, and glycolipids, (ii) peptides based on the primary sequence of the carbohydrate binding site, (iii) anti-selectin antibodies, (iv) oligosaccharides related to $Lewis^X$, (v) inositol polyanions and sulfated sugars, (vi) heparin, and (vii) molecular mimics of sLe^X, including oligonucleotides (reviewed in Refs. 2 and 3). Analogs of acceptor substrates of the various glycosyltransferases involved in glycan biosynthesis provide another class of potential inhibitors (reviewed in Refs. 4 and 5). Although many of these analogs are effective *in vitro*, they generally do not exhibit inhibitory activity in cells due to poor membrane permeability. The large number of polar hydroxyl groups and the lack of membrane transporters for oligosaccharides in most cells presumably prevent their uptake (6).

In contrast to many of the inhibitors described above, peracetylated disaccharides (*e.g.* acetylated Galβ1–4GlcNAcβ-*O*-naphthalenemethanol (NM), acetylated Galβ1–3GalNAcα-O-NM, and acetylated GlcNAcβ1–3Galβ-O-NM) inhibit sLe^X biosynthesis in cells (6–9). These compounds are taken up by cells by passive diffusion and acted on by cytoplasmic or membrane-associated carboxyesterases, which remove the acetyl groups. The compounds gain access to the biosynthetic enzymes located in the Golgi complex, where they serve as substrates, priming oligosaccharide synthesis and generating products related to *O*-GalNAc-linked mucin oligosaccharides. Priming in this manner diverts the assembly of the *O*-linked chains from endogenous glycoproteins, resulting in inhibition of expression of terminal Lewis antigens that are recognized by

* This work was supported, in whole or in part, by National Institutes of Health Grants CA46462 and CA112278 (to J. D. E.) and by the Intramural Research Program of the National Institutes of Health, NCI, Center for Cancer Research. The crystallographic part of this project has been funded, in whole or in part, with federal funds from NCI, National Institutes of Health, under Contract N01-CO-12400. The costs of publication of this article were defrayed in part by the payment of page charges. This article must therefore be hereby marked "*advertisement*" in accordance with 18 U.S.C. Section 1734 solely to indicate this fact.

The atomic coordinates and structure factors (code 3EE5) have been deposited in the Protein Data Bank, Research Collaboratory for Structural Bioinformatics, Rutgers University, New Brunswick, NJ (http://www.rcsb.org/).

[S] The on-line version of this article (available at http://www.jbc.org) contains supplemental Table 1.

[1] Present address: Zacharon Pharmaceuticals Inc., 505 Coast Blvd. S., La Jolla, CA 92037.

[2] To whom correspondence should be addressed: Dept. of Cellular and Molecular Medicine, University of California, San Diego, La Jolla, CA 92093. Tel.: 858-822-1100; Fax: 585-534-5611; E-mail: jesko@ucsd.edu.

[3] The abbreviations used are: sLe^X, sialyl Lewis X; NM, naphthalenemethanol; LLC, Lewis lung carcinoma; MES, 4-morpholineethanesulfonic acid; HPLC, high pressure liquid chromatography; β4Gal-T1, β1–4-galactosyltransferase 1.

selectins. Inhibition occurs at a much lower dose than for monosaccharide-based agents, such as GalNAcβ-*O*-benzyl (~25 μM *versus* 1–2 mM, respectively) (10, 11). Furthermore, the disaccharides appear to selectively affect sLe^X formation, since sLe^a expression was unaffected (12). By blocking selectin ligand expression, these compounds block both experimental and spontaneous metastasis (12, 13).

In this study, we have examined acetylated disaccharide analogs that have been modified so that after deacetylation their activity as substrates would be altered. Characterization of the 4′-deoxy derivative using β1–4-galactosyltransferase 1 as a model showed that it acts by competitively inhibiting the enzyme. Interestingly, the peracetylated form of this analog maintains the capacity to inhibit sLe^X expression in U937 lymphoma cells and Lewis lung carcinoma (LLC) cells and block tumor formation *in vivo*. Thus, the deoxy analog presumably inhibits one or more galactosyltransferases *in vivo*, thereby blocking sLe^X formation and experimental tumor cell metastasis without generation of oligosaccharide products.

EXPERIMENTAL PROCEDURES

General Chemical Methods—Optical rotations were measured at room temperature using an Autopol III polarimeter or a PerkinElmer Life Sciences 241-Mc polarimeter. Melting points were measured with Unimet Thomas Hoover. NMR experiments were carried out on a Bruker AMX-300, AMX-400, AMX-500, or Varian Mercury 400-MHz spectrometer. Chloroform was used as an internal standard for chemical shift calibration unless otherwise noted; the ^1H chemical shift of $CHCl_3$ was set to 7.262 ppm, and the ^{13}C chemical shift of CDCl3 was set to 77.0 ppm. Mass spectrometric data were recorded using Electrospray API-100, Electrospray LCQDECA, or FAB with 3-nitrobenzyl alcohol as the matrix and polyethylene glycol as the reference. All reaction products were analyzed by thin layer chromatography on Silica Gel 60-F_{254} (Merck) plates and detection by UV light or by charring with 5% (v/v) H_2SO_4 in ethanol. Column chromatography was performed on Silica Gel 60 (40–63 mm; Mallinckrodt V 150). Molecular sieves (4A) were heated at 180 °C for 24 h prior to use. All solvents were distilled prior to use and stored over molecular sieves. Chemical reactions were performed in oven-dried glassware under an inert argon atmosphere. All evaporations were carried out at 40–50 °C under reduced pressure, unless otherwise noted.

Chemical Synthesis of C-3′- and C-4′ Hydroxyl-modified Glycosides—Disaccharide **1** was prepared as described (8). Per-*O*-acetylated 4-deoxy-GlcNAcβ1–3Galβ-*O*-NM (**2**), per-*O*-acetylated 4-fluoro-GlcNAcβ1–3Galβ-*O*-NM (**3**), per-*O*-acetylated 4-azido-GlcNAcβ1–3Galβ-*O*-NM (**4**), per-*O*-acetylated 4-amino-GlcNAcβ1–3Galβ-*O*-NM (**5**), per-*O*-acetylated 4-methoxy-GlcNAcβ1–3Galβ-*O*-NM (**6**), per-*O*-acetylated 3-deoxy-GlcNAcβ1–3Galβ-*O*-NM (**7**), per-*O*-acetylated 3-fluoro-GlcNAcβ1–3Galβ-*O*-NM (**8**), and per-*O*-acetylated 3-methoxy-GlcNAcβ1–3Galβ-*O*-NM (**9**) were chemically synthesized and characterized by NMR spectroscopy and mass spectrometry as outlined below. The data were in good accordance with the proposed structures.

2-Naphthylmethyl 2-acetamido-3,6-di-*O*-acetyl-2,4-dideoxy-β-D-glucopyranosyl-(1,3)-2,4,6-tri-*O*-acetyl-β-D-galactopyranoside (**2**) (100 mg, 87%). ^1H NMR (400 MHz, $CDCl_3$): δ 7.84-7.28 (m, 7 H, Ar), 5.51 (d, 1 H, J = 8 Hz, NH), 5.37 (d, 1 H, J = 3.2 Hz, H-4), 5.21 (m, 2 H, H-2, H-3′), 5.02 (d, 1 H, J = 12.4 Hz, $ArCH_2$), 4.77 (d, 1 H, J = 12.5 Hz, $ArCH_2$), 4.76 (d, 1 H, J = 7.6 Hz, H-1′), 4.43 (d, 1 H, J = 7.6 Hz, H-1), 4.16-4.04 (m, 4 H, H-6 × 4), 3.80-3.76 (m, 2 H, H-3, H-5), 3.66 (m, 1 H, H-5′), 3.28 (m, 1 H, H-2′), 2.13, 2.09, 2.06, 2.05, 2.01 (5s, 15 H, CH_3CO), 2.03 (m, 1 H, H-4′b), 1.90 (s, 3 H, NHAc), 1.64 (q, 1 H, J = 12.4 Hz, H-4′a); ^{13}C NMR (100 MHz, $CDCl_3$): δ 170.91-169.85 (C=O), 134.49, 133.37, 133.28, 128.50, 128.06, 127.96, 127.06, 126.55, 126.39, 125.92 (10 C, Ar C), 100.54 (C-1′), 99.57 (C-1), 75.78 (C-3), 71.55 (C-2), 71.26 (C-5), 70.70 ($ArCH_2$), 69.67 (C-4), 69.64 (C-3′), 69.29 (C-5′), 65.33 (C-6′), 62.42 (C-6), 56.49 (C-2′), 33.26 (C-4′), 23.57 (CH_3CON), 21.31-20.99 (5 C, CH_3COO). $[\alpha]_D$ −37.7° (c 0.135; $CHCl_3$). HRMS FAB Calcd for $[C_{35}H_{43}NO_{15}]$ [M + H^+]: m/z 718.2711. Found [M + H^+]: m/z 718.2717.

2-Naphthylmethyl 2-acetamido-3,6-di-*O*-acetyl-2,4-dideoxy-4-fluoro-β-D-glucopyranosyl-(1,3)-2,4,6-tri-*O*-acetyl-β-D-galactopyranoside (**3**) (28 mg, 79%). ^1H NMR (500 MHz, $CDCl_3$): δ 7.83-7.78 (m, 3 H, Ar), 7.71 (br s, 1 H, Ar), 7.48-7.46 (m, 2 H, m, Ar), 7.37 (dd, 1 H, J = 8.5, 1.9 Hz, Ar), 5.58 (d, 1 H, J = 8.1 Hz, NH), 5.49-5.42 (m, 1H), 5.32 (d, 1 H, d, J = 3.0 Hz, H-4), 5.18 (dd, 1 H, J = 9.9, 7.7 Hz, H-3), 5.0 (d, 1 H, J = 15.0 Hz, $ArCH_2$), 4.86 (d, 1 H, J = 8.1, H-1′), 4.76 (d, 1 H, J = 15.0 Hz, $ArCH_2$), 4.57 (dr d, 1 H, J = 10.3 Hz), 4.46 (dt, 1 H, J = 4.2, 9.2 Hz, H-4′), 4.41 (d, 1 H, J = 8.1 Hz, H-1), 4.12 (d, 2 H, J = 6.6 Hz, H_2-6), 4.08-4.04 (m, 1 H), 3.78-3.73 (m, 2 H, H_2-6′), 3.63-3.60 (m, 1 H, H-5′), 3.40-3.34 (m, 1 H, H-5), 2.10, 2.09, 2.08, 2.05, 2.03 and 1.87 (s, 3 H each, Ac × 6). ^{13}C NMR (125 MHz, $CDCl_3$): δ 170.66, 170.59, 170.50, 170.43, 169.84, 169.49, 134.15, 133.11, 133.02, 128.25, 127.79, 127.70, 126.83, 126.30, 126.15, 125.66, 99.90, 99.21, 86.83 (d, J = 18.7 Hz, C-4′), 76.08, 71.01 (d, J = 11.6 Hz, C-3′), 71.18, 70.81, 70.46, 69.17, 62.01, 60.90, 55.38 (d, J = 6.7 Hz, C-2′), 20.96, 20.76, 20.72, 20.69, 20.68, 20.66. $[\alpha]_D$ −24.0° (c 0.1; $CHCl_3$). ESIMS Calcd for $[C_{35}H_{42}FNO_{15}]$ [M + Na^+]: m/z 758. Found [M + Na^+]: m/z 758.

2-Naphthylmethyl 2-acetamido-3,6-di-*O*-acetyl-4-azido-2,4-dideoxy-β-D-glucopyranosyl-(1,3)-2,4,6-tri-*O*-acetyl-β-D-galactopyranoside (**4**) (53 mg, 66%). ^1H NMR (400 MHz, $CDCl_3$): δ 7.85-7.38 (m, 7 H, Ar), 5.45 (1 H, NHAc), 5.33 (d, l H, J = 2.8 Hz, H-4), 5.27 (1 H, dd, J = 10.8, 9.6 Hz, H-3′), 5.20 (dd, 1 H, J = 10, 8 Hz, H-2), 5.03 (d, 1 H, J = 12.4 Hz, $ArCH_2$), 4.78 (d, 1 H, J = 8.0 Hz, H-1′), 4.77 (d, 1 H, J = 12.4 Hz, $ArCH_2$), 4.57 (dd, 1 H, J = 12.0, 2.4 Hz, H-6b′), 4.42 (d, 1 H, J = 8 Hz, H-1), 4.15 (d, 2 H, J = 6.4 Hz, H-6a, H-6b), 4.07 (dd, l H, J = 12.4, 3.6 Hz, H-6a′), 3.76 (t, 1 H, J = 6.4 Hz, H-5), 3.75 (dd, 1 H, J = 10, 3.6 Hz, H-3), 3.61 (t, 1 H, J = 10 Hz, H-4′), 3.44 (dt, 1 H, J = 10, 8.4 Hz, H-2′), 3.34 (m, 1 H, H-5′), 2.13, 2.12, 2.11, 2.10, 2.05, 1.89 (s, 3 H each, Ac × 6). ^{13}C NMR (100 MHz, $CDCl_3$): δ 174.42, 170.86, 170.71, 170.70, 170.12, 169.73, 135.71, 134.42, 133.36, 128.51, 128.07, 127.97, 127.11, 126.58, 126.42, 125.94, 100.27 (C-1′), 99.45 (C-1), 76.16 (C-3), 72.81 (C-2), 72.29 ($ArCH_2$), 71.43 (C-5), 71.13, 70.71, 69.41, 62.26, 61.87, 60.39, 55.76, 23.40, 21.77, 20.98 (4C). $[\alpha]_D$ +18.0° (c 1.0; $CHCl_3$). HRMS FAB Calcd for $[C_{35}H_{42}N_40_{15}]$; m/z 758.2641; Found: m/z 758.2652.

2-Naphthylmethyl 2-acetamido-3,6-di-*O*-acetyl-4-amino-2,4-dideoxy-β-D-glucopyranosyl-(1,3)-2,4,6-tri-*O*-acetyl-β-D-galactopyranoside (**5**) (9 mg, 94%). ^{1}H NMR (400 MHz, $CDC1_3$): δ 7.84-7.38 (m, 7 H, Ar), 6.15 (l H, NHAc), 5.36 (m, 2 H, H-4, H-3′), 5.22 (dd, l H, *J* = 10, 8 Hz, H-2), 5.03 (d, l H, *J* = 12.4 Hz, $ArCH_2$), 4.77 (d, 1 H, *J* = 12.4 Hz, $ArCH_2$), 4.76 (d, 1 H, *J* = 7.6 Hz, H-1′), 4.44 (d, 1 H, *J* = 8.0 Hz, H-1), 4.1–4.3 (m, 3 H), 3.2–3.8 (m, 6 H), 1.85–2.14 (18 H). ^{13}C NMR (100 MHz, $CDC1_3$): δ 172.12, 171.58, 170.73, 170.74, 170.27, 169.64, 134.38, 133.27, 133.18, 128.39, 127.9 6, 127.86, 127.00, 126.93, 126.46, 126.30, 125.79, 100.12 (C-l′), 99.43 (C-1), 76.48 (C-3), 71.46 (C-2), 70.91 (C-5), 70.64 ($ArCH_2$), 69.34 (C-4), 69.21 (C-37, 62.53 (C-6′), 62.30 (C-6), 62.13 (C-5′), 51.30 (C-2′), 46.60 (C-4′), 23.31, 23.16, 22.87, 21.20, 20.98, 20.90. $[\alpha]_D$ + 17.0° ($CHC1_3$). HRMS FAB Calcd for $[C_{35}H_{45}N_20_{15}]$ [M + H^+]: *m*/*z* 733.2814. Found: *m*/*z* 733.2821.

2-Naphthylmethyl 2-acetamido-3,6-di-*O*-acetyl-2,4-dideoxy-4-methoxy-β-D-glucopyranosyl-(1,3)-2,4,6-tri-*O*-acetyl-β-D-galactopyranoside (**6**) (22 mg, 66%). ^{1}H NMR (400 MHz, $CDC1_3$): δ 7.85–7.37 (m, 7 H, Ar), 5.41 (1 H, NHAc), 5.34 (d, 1 H, *J* = 3.2 Hz, H- 4), 5.20 (dd, 1 H, *J* = 10, 8 Hz, H-2), 5.10 (dd, l H, *J* = 10.4, 8.8 Hz, H-3′), 5.03 (d, 1 H, *J* = 12.4 Hz, $ArCH_2$), 4.76 (d, 1 H, *J* = 12.4 Hz, $ArCH_2$), 4.62 (d, 1 H, *J* = 8.0 Hz, H-1), 4.54 (dd, l H, *J* = 12.4, 2.8 Hz, H-6b), 4.42 (d, 1 H, *J* = 7.6 Hz, H-1′), 4.15 (d, 2 H, *J* = 6.4 Hz, H-6a′, H-6b′), 4.06 (dd, 1 H, *J* = 12.4, 3.6 Hz, H-6a), 3.78 (t, 1 H, *J* = 6.4 Hz, H-5′), 3.74 (dd, 1 H, *J* = 10, 3.6 Hz, H-3), 3.57 (m, 1 H, H-5), 3.41 (s, 3 H, OMe), 3.32 (dd, 1 H, *J* = 8.8, 7.6 Hz, H-2′), 2.13, 2.12, 2.10, 2.07, 2.04, and 1.89 (s, 3 H each, Ac × 6). ^{13}C NMR (100 MHz, $CDC1_3$): δ 171.06, 170.50, 170.20, 169.59, 134.48, 133.38, 133.29, 128.50, 128.07, 127.96, 127.09, 126.55, 126.39, 125.95, 100.68, (C-1′), 99.47 (C-1), 78.19 (C-4′), 76.01 (C-2′), 74.30, 73.13, 71.48, 71.23, 70.67, 69.47, 62.35, 61.91, 60.56, 55.25, 28.51, 23.40, 21.26, 21.15, 21.14, 20.99. $[\alpha]_D$ −12.0° ($CHC1_3$). HRMS FAB Calcd for $C_{36}H_{45}N0_{16}$; *m*/*z* 747.2733. Found: *m*/*z* 747.2731.

2-Naphthylmethyl 2-acetamido-4,6-di-*O*-acetyl-2,3-dideoxy-β-D-glucopyranosyl-(1,3)-2,4,6-tri-*O*-acetyl-β-D-galactopyranoside (**7**) (95 mg, 76%). ^{1}H NMR (500 MHz, $CDCl_3$): δ 7.83-7.79 (m, 3 H, Ar), 7.72 (br s, 1 H, Ar), 7.49-7.47 (m, 2 H, Ar), 7.40-7.37 (dd, 1 H, *J* = 8.52, 1.5 Hz, Ar), 5.76 (d, 1 H, *J* = 6.5 Hz, NH), 5.34 (d, 1 H, *J* = 3.2 Hz, H-4), 5.20 (dd, 1 H, *J* = 10, 8.3 Hz, H-3), 5.02 (d, 1 H, *J* = 12.3 Hz, $ArCH_2$), 4.78 (d, 1 H, *J* = 12.3 Hz, $ArCH_2$), 4.77 (d, 1 H, *J* = 7.9 Hz, H-1′), 4.78-4.70 (m, 1 H), 4.44 (d, 1 H, *J* = 7.9 Hz, H-1), 4.28 (dd, 1 H, *J* = 12.0, 3.3 Hz, H-6′), 4.14 (dd, 2 H, *J* = 6.7, 2.9 Hz), 4.02 (dd, 1 H, *J* = 12, 4.7 Hz, H-6′), 3.79-3.75 (m, 2 H), 3.62-3.58 (m, 1 H, H-5′), 3.28-3.24 (m, 1 H, H-5), 2.45-2.39 (m, 1 H, H-4′), 2.12, 2.08, 2.06, 2.05, 2.00, and 1.91 (s, 3H each, Ac × 6). ^{13}C NMR (100 MHz, $CDCl_3$): δ 170.80, 170.62, 170.46, 169.98, 169.85, 169.51, 134.16, 133.10, 133.04, 128.28, 127.82, 127.74, 126.87, 126.34, 126.19, 125.69, 100.89, 99.21, 75.67, 74.76, 71.27, 71.10, 70.53, 69.24, 66.33, 62.05, 50.49, 30.96, 24.92, 23.89, 21.06, 20.94, 20.83, 20.77. $[\alpha]_D$ −10.2° (c 0.25; $CHCl_3$). ESIMS Calcd for $[C_{35}H_{43}NO_{15}]$ [M + Na^+]: 740. Found [M + Na^+]: *m*/*z* 740.

2-Naphthylmethyl 2-acetamido-4,6-di-*O*-acetyl-2,3-dideoxy-3-fluoro-β-D-glucopyranosyl-(1,3)-2,4,6-tri-*O*-acetyl-β-D-galactopyranoside (**8**) (32 mg, 41%). ^{1}H NMR (500 MHz, $CDCl_3$): δ 7.82-7.78 (m, 3 H, Ar), 7.70 (br s, 1 H, Ar), 7.49-7.45 (m, 2 H, Ar), 7.37 (dd, 1 H, *J* = 8.5, 1.5 Hz, Ar), 6.01 (d, 1 H, *J* = 5.0 Hz, NH), 5.34 (d, 1 H, *J* = 3.3 Hz, H-4), 5.26-5.12 (m, 2 H, H-3′,H-4′), 5.22 (d, 1 H, *J* = 7.7 Hz, H-1′), 5.08–5.0 (m, 1 H), 5.01 (d, 1 H, *J* = 15 Hz, $ArCH_2$), 4.75 (d, 1 H, *J* = 15 Hz, $ArCH_2$), 4.41 (d, 1 H, *J* = 7.7 Hz, H-1), 4.27 (br d, 1 H, *J* = 11.7 Hz, H-6), 4.17-4.08 (m, 2 H), 4.02 (dd, 1 H, *J* = 12.5, 4.0 Hz), 3.77-3.73 (m, 2 H), 3.55 (br dt, 1 H, *J* = 9.9 Hz), 2.94-2.91 (m, 1 H), 2.11 (s, 6 H, Ac × 2), 2.07, 2.05, 2.01, and 1.94 (s, 3 H each, Ac × 4). ^{13}C NMR (125 MHz, $CDCl_3$): δ 171.09, 170.66, 170.56, 169.71, 169.68, 169.38, 134.13, 133.08, 133.02, 128.25, 127.78, 127.69, 126.80, 126.29, 126.14, 125.62, 99.32 (C-1), 98.33 (d, *J* = 10.1 Hz, C-1′), 88.71 (d, *J* = 179.7 Hz, C-3′), 76.43, 71.27, 70.59, 70.52, 70.49, 69.37, 69.0 (d, *J* = 17.5 Hz, C-4′), 62.04, 61.12, 58.40 (d, *J* = 16.5 Hz, C-2′), 23.40, 20.93, 20.74, 20.71, 20.68, 20.64. $[\alpha]_D$ −12.0° (c 0.1; $CHCl_3$). ESIMS Calcd for $[C_{35}H_{42}NFO_{15}]$ [M + Na^+]: *m*/*z* 758. Found [M + Na^+]: *m*/*z* 758.

2-Naphthylmethyl 2-acetamido-4,6-di-*O*-acetyl-2,3-dideoxy-3-methoxy-β-D-glucopyranosyl-(1,3)-2,4,6-tri-*O*-acetyl-β-D-galactopyranoside (**9**) (83 mg, 79%). ^{1}H NMR (400 MHz, $CDC1_3$): δ 7.35–7.85 (m, 7 H, Ar), 6.00 (d, 1 H, d, *J* = 7.2 Hz, NHAc), 5.35 (d, 1 H, *J* = 3.2 Hz, H-4), 5.20 (dd, l H, *J* = 9.6, 8 Hz, H-2), 5.15 (d, 1 H, *J* = 8.4 Hz, H-1′), 5.03 (d, 1 H, *J* = 12.4 Hz, $ArCH_2$), 4.87 (t, 1 H, *J* = 10 Hz, H- 4′), 4.77 (d, 1 H, *J* = 12.4 Hz, $ArCH_2$), 4.42 (d, 1 H, *J* = 8 Hz, H-1), 4.23-3.99 (m, 5 H), 3.70–3.79 (m, 3 H), 3.52 (m, 1 H, H-5), 3.37 (s, 3 H, OMe), 2.11 (s, 3 H, Ac × 1), 2.08 (s, 3 H, Ac × 1), 2.05 (s, 9 H, Ac × 3), 1.94 (s, 3 H, Ac × 1). ^{13}C NMR (100 MHz, $CDC1_3$): δ 171.25, 170.99, 170.83, 169.98, 169.78, 134.46, 133.36, 133.28, 128.490, 128.05, 127.96, 127.06, 126.54, 126.39, 125.91, 99.63 (C-1), 99.24 (C-1′), 78.20 (C-3′), 76.43 (C-3), 71.93, 71.61, 70.89, 70.73, 69.73, 62.38, 61.95, 60.19, 58.77, 23.76, 21.25, 21.09, 21.04, 21.03, 20.97. $[\alpha]_D$ −13.0° ($CHCl_3$). HRMS FAB Calcd for $C_{36}H_{45}N0_{16}$: *m*/*z* 747.2733. Found: *m*/*z* 747.2747.

Crystallization and Data Collection— hM340H/C338T-β1–4Gal-T1 was described previously (15). The crystals of the protein-acceptor complex were grown by the hanging droplet method. An equal volume of the mutant protein solution (10–20 mg/ml protein) was mixed with 10 mM $MnCl_2$, 10 mM UDP-hexanolamine (Sigma), and 0.1 mM deacetylated disaccharide **1** (GlcNAcβ1–3Galβ-*O*-NM). The precipitant contained MES-NaOH buffer (pH 6.0), 1.5 M ammonium sulfate, and 3% dioxane. Crystals grew in 1–2 weeks and diffracted up to 2.2 Å resolution. The three-dimensional x-ray diffraction data were collected on a single crystal at 100 K on an in-house x-ray rotating anode generator with a Mar345 detector (Macromolecular Crystallographic Laboratory, NCI, National Institutes of Health). The frames were processed and scaled using HKL2000 (15). Since the crystal was isomorphous with the earlier solved crystal structure of the same protein in the presence of various acceptor substrates, its protein coordinates (Protein Data Bank entry 2AEC) were used to solve the present crystal structure (15). The final refinement statistics are listed in supplemental Table 1. All of the refinements were carried out by CNS1.0 (16), and the density fittings were done using the computer program O (17). All crystal structures were drawn with PyMol (18). Crystallization of the same complex using deacetylated analog **2** has not yet yielded suitable crystals for x-ray data collection.

Cell Lines, Radiolabeling, and HPLC Analysis of Oligosaccharides—U937 cells (CRL 1593.2) and murine LLC cells (LLC1, CRL-1642) were purchased from the American Type Culture Collection (Manassas, VA) and cultured in Dulbecco's modified Eagle's medium supplemented with 10% (v/v) fetal bovine serum (Hyclone Laboratories, Logan, UT), glutamine (0.3 g/liter), streptomycin sulfate (100 μg/ml), and penicillin (100 units/ml). Cells were maintained at 37 °C in a humidified incubator containing 5% CO_2 and 95% air and passaged every 4 days using ATV^{TM} trypsin solution (Invitrogen). The various disaccharides were dissolved in Me_2SO and added to growth medium to achieve the indicated concentrations. The final concentration of Me_2SO was adjusted to 0.5% (v/v) in all samples. Cells were added to the supplemented medium at a density of 2×10^5 cells/ml.

[6-^{3}H]Fucose (85.2 Ci/mmol) and [6-^{3}H]galactose (29.5 Ci/mmol) were purchased from PerkinElmer Life Sciences. Cells were radiolabeled in growth medium containing 1 mM glucose. Samples of radiolabeled oligosaccharide products were analyzed by reverse phase HPLC as described (9). Nonradioactive samples were analyzed by mass spectrometry on a Thermo Finnigan LCQ classic mass spectrometer (San Jose, CA). Samples in water (10 μl) were introduced into the electrospray ionization ion trap using an autosampler connected to a TSP P400 quaternary pump using 50% acetonitrile containing 0.1% formic acid.

Enzyme-linked Immunosorbent Assay and Galactosyltransferase Assays—To measure the presence of sLe^X and P-selectin ligand, cells were grown to confluence for 3–4 days in 6-well plates with and without **1–9**. Binding of monoclonal antibody CSLEX-1 and P-selectin Ig chimera to cells fixed with 1% paraformaldehyde was measured by an enzyme-linked immunosorbent assay as described (9, 13). Background binding was measured after treatment with sialidase, which showed that nonspecific binding was less than 5%.

The standard galactosyltransferase reaction (25 μl) contained 10 milliunits of purified bovine milk β1–4-galactosyltransferase (Sigma), 50 mM MES, pH 6.0, 0.3 μCi of UDP-[1-^{3}H]galactose, 250 μM UDP-galactose, 15 mM $MnCl_2$, 50 mM KCl, and varying amounts of deacetylated **1** as acceptor. After incubation at room temperature for 15 min, the reaction products were diluted with 1 ml of 0.5 M NaCl and applied to a Sep-Pak C18 (100 mg; Waters). After washing with 5 ml of water, the products were eluted with 50% methanol, dried, and counted by liquid scintillation. Ovalbumin was tested as substrate at 10 mg/ml as described (19). The inhibitory activities of deacetylated **1** and **2** were tested at the indicated concentrations.

Experimental Metastasis—LLC cells were grown for 4–5 days in the presence or absence of 50 μM **1** or **2**. The cells were harvested with EDTA, resuspended in sterile 0.9% saline, and injected (2×10^5 cells/150 μl) into the lateral tail vein of anesthetized (inhaled isoflurane, Janssen Pharmaceuticals, Titusville, NJ) 8–12-week-old Es1(e) mice (bred in a C57Bl/6 background, a kind gift from P. Potter, University of North Carolina via Charles River Laboratories) (20). These mice carry a mutant allele of the esterase locus Es-1 designated Es1(e) (21) that results in reduced plasma esterase activity (22). After 10 days, lung metastases were detected by visible nodules on the surface of the lungs and quantitated under a dissecting microscope. Representative photographs were taken.

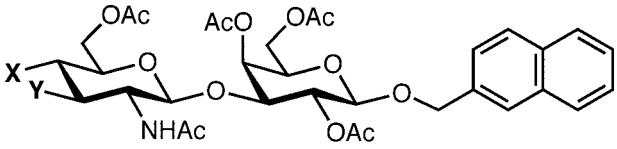

1 **X**=OAc, **Y**=OAc
2 **X**=H, **Y**=OAc
3 **X**=F, **Y**=OAc
4 **X**=N_3, **Y**=OAc
5 **X**=NH_2, **Y**=OAc
6 **X**=OCH_3, **Y**=OAc
7 **X**=OAc, **Y**=H
8 **X**=OAc, **Y**=F
9 **X**=OAc, **Y**=OCH_3

FIGURE 1. **Chemical structure of per-*O*-acetylated GlcNAcβ1–3Galβ-*O*-naphthalenemethanol (1) and C-3′ and C-4′ hydroxyl-modified analogs (2–9).**

RESULTS AND DISCUSSION

GlcNAcβ1–3Galβ-O-NM Binds to β1–4-Galactosyltransferase 1—We have shown previously that disaccharide **1** (peracetylated GlcNAcβ1–3Galβ-*O*-NM) acts as an inhibitor of sLe^X biosynthesis when provided to cultured tumor cells (Fig. 1) (6–9). In order for **1** to be active, it first undergoes carboxyesterase-catalyzed esterolysis, which results in removal of the acetate groups required for making the compound membrane-permeable (6). Deacetylated **1** then serves as a substrate for galactosylation catalyzed by one or more galactosyltransferases expressed by cells (23), and the galactosylated trisaccharide product (presumably Galβ1–4GlcNAcβ1–3Galβ-*O*-NM) can then undergo sialylation, fucosylation, or the addition of another *N*-acetylglucosamine residue (9). Although deacetylated **1** could act as a substrate for several galactosyltransferases, in this study, we chose β1–4-galactosyltransferase 1 (β4Gal-T1) as a model to examine the properties of analogs of **1**.

β4Gal-T1 forms Galβ1–4GlcNAc units in various glycoconjugates and has been shown to participate in the formation of sLe^X and selectin ligands (24). Human β4Gal-T1 has been studied by x-ray crystallography, which has led to detailed insights into its kinetic mechanism (25–27). To determine how deacetylated **1** interacts with β4Gal-T1, we co-crystallized it with the open form of the human enzyme, hM340H-Gal-T1, in the presence of Mn^{2+} and UDP-hexanolamine (Fig. 2*a*) (15, 28, 29). The apo-β4Gal-T1 enzyme exists in an open conformation, where the acceptor binding site is absent. Upon binding of Mn^{2+} and UDP-Gal, but not UDP and Mn^{2+}, the wild type β4Gal-T1 undergoes conformational changes that create the acceptor binding site (29). It has been shown that mutation of the Met-344 residue in bovine β4Gal-T1 (corresponding residue Met-340 in human β4Gal-T1) to a His residue can facilitate these conformational changes readily in the presence of Mn^{2+} and UDP-hexanolamine, creating the acceptor binding site (28). Therefore, in the past (15, 28) and in the present crystallographic studies, instead of wild-type human β4Gal-T1, the

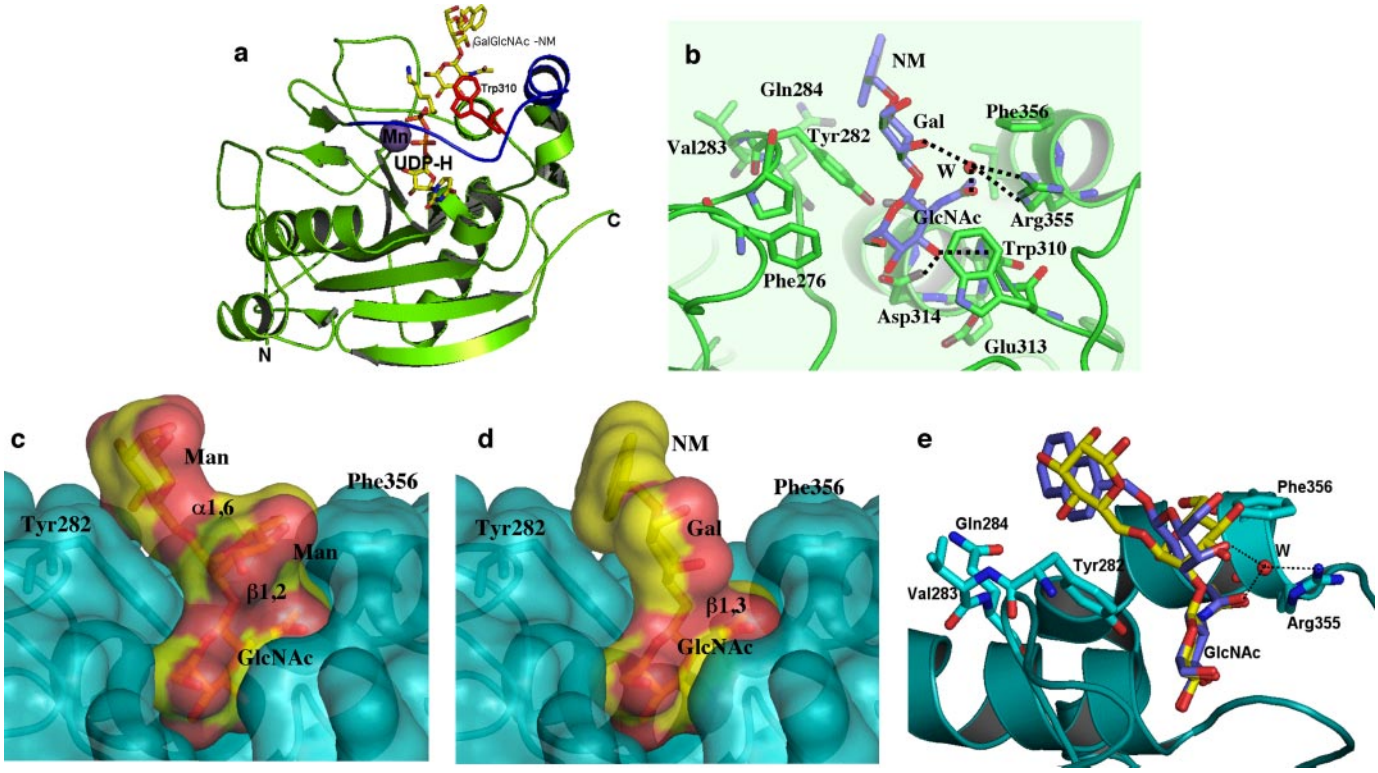

FIGURE 2. **Co-crystallization of deacetylated 1 with the open form of the human enzyme, hM340H-Gal-T1.** *a*, binding of deacetylated **1** to the catalytic domain of β4Gal-T1, in the presence of Mn^{2+} (*purple sphere*) and UDP-hexanolamine (*UDP-H*). The β4Gal-T1 molecule is found in the closed conformation with its Trp-310 side chain (*red*) placed inside the catalytic pocket, interacting with the phosphate oxygen atom of UDP-hexanolamine molecule, whereas the long flexible loop (*blue*) covers the UDP-hexanolamine and exposes the acceptor binding site to facilitate binding to the enzyme. *b*, the molecular interactions of deacetylated **1** (*blue*) with the β4Gal-T1 (*green*). The hydrogen bonds are shown in *black dotted lines*. The GlcNAc moiety of deacetylated **1** is bound in the acceptor sugar binding site. The Gal residue forms hydrophobic interactions with the aromatic side chain of the Tyr-282 residue, whereas the naphthalenemethanol extends out of the sugar binding site, weakly interacting with the β4Gal-T1 molecule. There is a structural water molecule (*W*) indicated with *black dotted lines* that, in addition to forming a hydrogen bond with the side-chain amino group of Arg-355, bridges the GlcNAc and Gal via hydrogen bonds. *c*, molecular surface (van der Waals) diagram showing the binding of deacetylated trisaccharide GlcNAcβ1–2Manα1–6Manβ-*O*-R (where R represents -CH_2–CH_2–CH_2–CH=CH_2 (15)) to β4Gal-T1 (*light blue*). *d*, molecular surface (van der Waals) diagram showing the binding of deacetylated disaccharide **1** to β4Gal-T1 (*light blue*). *e*, superposition of the bound deacetylated disaccharide **1** (*blue*) with the bound trisaccharide, GlcNAcβ1–2Manα1–6Manβ-*O*-R (*yellow*) in the respective acceptor substrate complexes with β4Gal-T1 (*blue*).

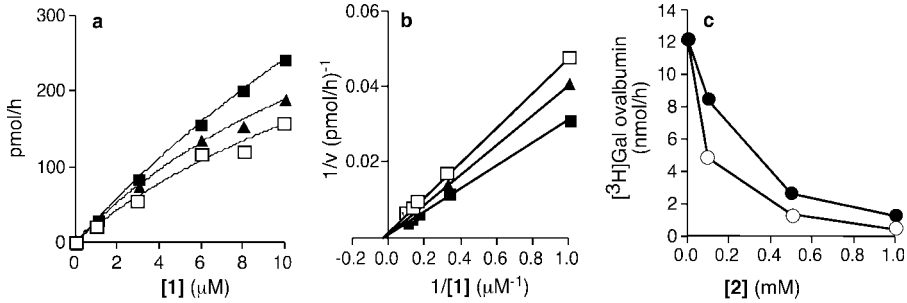

FIGURE 3. **Competitive inhibition of β4GalT-1 by deacetylated 2.** *a*, inhibition of β4GalT-1 activity by deacetylated **2** was measured with different concentrations of deacetylated **1** in the absence (*filled squares*) or presence of deacetylated **2** (150 μM (*filled triangles*) and 300 μM (*open squares*)). *b*, replotting the data in reciprocal fashion showed that deacetylated **2** acted as a competitive inhibitor of deacetylated **1**. *c*, both deacetylated **1** (*filled circles*) and deacetylated **2** (*open circles*) inhibited the transfer of [^{3}H]galactose from UDP-[^{3}H]galactose to ovalbumin.

mutant hM340H-Gal-T1 in the presence of Mn^{2+}, UDP-hexanolamine was used to determine the acceptor substrate binding to β4Gal-T1. In the presence of deacetylated **1**, β4Gal-T1 was found in closed conformation with the Trp-310 side chain inside the catalytic pocket interacting with the bound UDP-hexanolamine (Fig. 2*a*). The long flexible loop in this structure is also found in the closed conformation, with His-343 coordinated with Mn^{2+} covering the UDP-hexanolamine and exposing the acceptor-substrate binding site to facilitate the binding of deacetylated **1**. The *N*-acetylglucosamine residue of deacetylated **1** is tightly bound in the acceptor sugar-binding site, and the β-linked galactose residue hydrophobically stacks on the aromatic side chain of Tyr-282 (Fig. 2*b*). The aglycone (naphthalenemethanol) extends out from the binding site. A structural water molecule forms a hydrogen bond with the side-chain amino group of Arg-355 as well as between the *N*-acetylglucosamine and galactose residues stabilizing the complex (Fig. 2*b*). A molecular surface depiction shows the similarity of binding of deacetylated **1** and the more natural substrate analog, GlcNAcβ1–2Manα1–6Manβ- (Fig. 2, *c*–*e*).

Deacetylated **1** (GlcNAcβ1–3Galβ-*O*-NM) acted as a substrate exhibiting an apparent K_m of ~10 μM (Fig. 3*a*), a value lower than that reported for GlcNAcβ1–2Manα1–6Man (K_m ~ 60 μM) (15). Although the GlcNAc moiety exhibits only

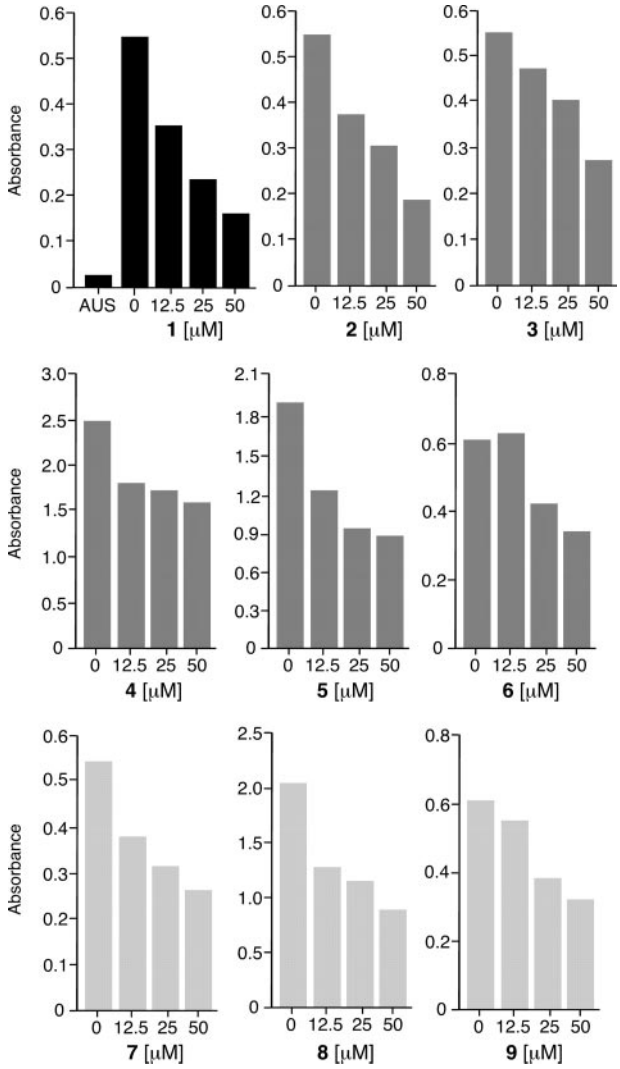

FIGURE 4. **Inhibition of sLe^X and β4GalT-1 by disaccharide analogs.** U937 cells were grown in the absence or presence of various concentrations of each peracetylated disaccharide analog for 4 days, as indicated. sLe^X was measured by an enzyme-linked immunosorbent assay using monoclonal antibody, CSLEX-1. The values represent the average of triplicate measurements, which varied by <10%. Treatment of control cells with *Arthrobacter ureafaciens* sialidase (*AUS*) abrogated binding of CSLEX-1. The *y* axis scale differs for various compounds because the individual compounds were tested in sets on different days. *Black bar graphs*, disaccharide **1**; *dark gray bar graphs*, C-4′ hydroxyl-modified analogs **2–6**; *light gray bar graphs*, C-3′ hydroxyl-modified analogs **7–9**.

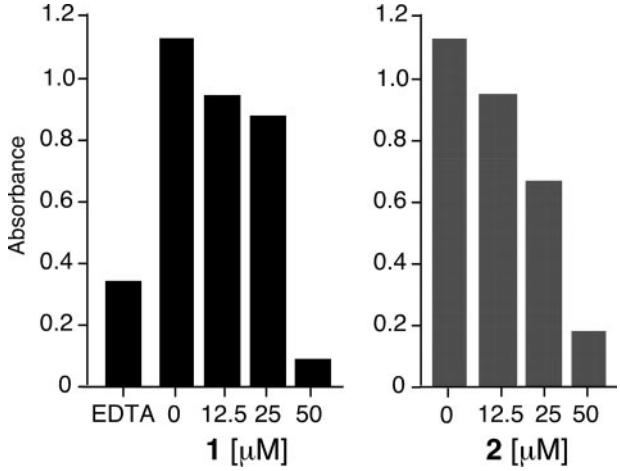

FIGURE 5. **Inhibition of P-selectin binding by disaccharide 1 and analog 2.** U937 cells were grown in the absence or presence of various concentrations of **1** or **2** for 4 days, as indicated. The binding of P-selectin-Ig chimera was measured by enzyme-linked immunosorbent assay, as described (13). The values represent the average of triplicate measurements, which varied by <10%. Treatment of control cells with 5 mM EDTA abrogated binding of P-selectin chimera due to its dependence on Ca^{2+}.

hydrophobic interactions with the β4Gal-T1 molecule (Fig. 2, *c* and *d*), the differences in the interaction of the galactose residue in deacetylated **1** *versus* the corresponding mannose residue in the trisaccharide substrate and additional contributions from the interaction of the naphthalenemethanol moiety with the enzyme may explain why deacetylated **1** has a lower K_m than that of GlcNAcβ1–2Manα1–6Man (Fig. 2*e*). Since β4GalT-1 transfer galactose to the C-4′ hydroxyl group of GlcNAc-containing acceptors, one would predict that the deacetylated 4′-deoxy derivative of **1** would not act as a substrate. As expected, this compound lacked acceptor activity (deacetylated **2**) when incubated with bovine β4GalT-I.

Previous studies showed that alterations of the C-4′ hydroxyl groups in acceptors for β4Gal-T1 (*i.e.* by deoxygenation, halogenation, alkylation, or amination of the *N*-acetylglucosamine residue) affected binding and reactivity of GlcNAc-containing substrates (14, 30–36). However, the enhanced interaction of deacetylated **1** with the enzyme compared with other substrates suggested that deacetylated **2** might act as a competitive inhibitor. As shown in Fig. 3*b*, deacetylated **2** acted as an inhibitor using deacetylated **1** as substrate. Replotting the data in reciprocal fashion (1/*v* *versus* 1/[S]) showed that it acted in a competitive manner with an apparent K_i of 192 ± 83 μM. Interestingly, both deacetylated **1** and **2** also inhibited the transfer of galactose to a glycoprotein substrate, ovalbumin, with comparable efficacy (Fig. 3*c*). These data differ from previous findings showing that 4-deoxy-GlcNAc-*O*-methyl or 4-deoxy-GlcNAcβ1–3Gal-*O*-methyl were not inhibitory (31, 33). One explanation for this discrepancy is that the large aromatic aglycone in deacetylated **2** compared with the *O*-Me group in previous derivatives may partially compensate for the loss of binding energy due to removal of the C-4′ hydroxyl group, perhaps by interaction with Tyr-282 in the acceptor binding site (Fig. 2*b*). The importance of the naphthalenemethanol moiety is also consistent with other studies showing that substrates containing aromatic aglycones can inhibit the enzyme from acting on free GlcNAc or GlcNAc-*O*-methyl with K_i values lower than K_m for GlcNAc (K_i = 10–22 μM *versus* K_m = 1–10 mM) (33, 34).

Acetylated Disaccharide Analogs Block sLe^X Formation in Tumor Cells—To test if the 4′-deoxy analog **2** had inhibitory activity *in vivo*, the compound was added to the culture medium of U937 human monocytic lymphoma-derived cells, and the expression of sLe^X on the cell surface was monitored with the monoclonal antibody CSLEX-1. Analog **2** diminished cell surface sLe^X expression in a dose-dependent manner and to a similar extent as the parent compound **1** (Fig. 4). The 4′-deoxy analog **2** also inhibited binding of a P-selectin-IgG chimera to cells in a dose-dependent manner similar to **1** with an ED_{50} value of ~30 μM (Fig. 5).

Since compound **2** lacks the acceptor hydroxyl group for galactosylation, in theory, any further modifications by fucosy-

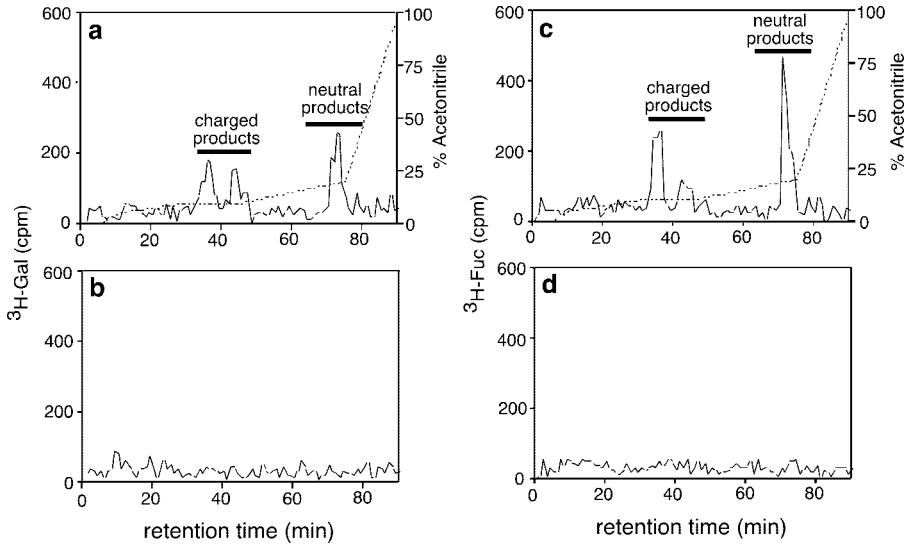

FIGURE 6. **Oligosaccharides were generated on deacetylated analog 1 but not on deacetylated analog 2.** U937 cells were incubated with 50 μM analog **1** or **2** for 4 days in the presence of 50 μCi/ml [^{3}H]Gal (*a* and *b*) or [^{3}H]Fuc (*c* and *d*). The radiolabeled products were extracted and separated by C18 reverse phase HPLC using a gradient of acetonitrile in water (*dashed line*). The *bars* indicate the elution positions of charged and neutral ^{3}H-labeled oligosaccharides, as defined previously (7, 9).

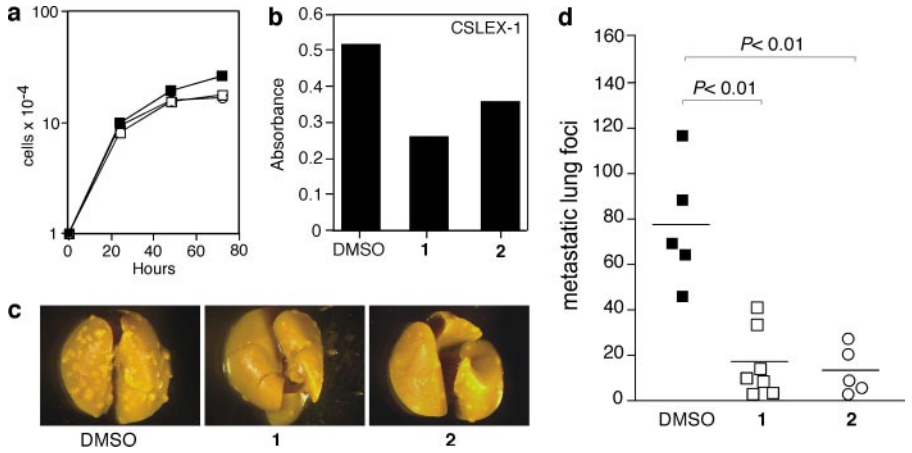

FIGURE 7. **Inhibition of experimental metastasis.** *a*, disaccharides **1** (*open squares*) and **2** (*open circles*) did not significantly affect the growth of LLC cells in culture compared with DMSO (*filled squares*). *b*, LLC cells were treated in culture with DMSO, 50 μM **1**, or 50 μM **2**. Both **1** and **2** inhibited sLe^X expression. The values represent the average of triplicate measurements, which varied by <10%. *c*, a single-cell suspension (2×10^5) of LLC cells was treated in culture with DMSO, 50 μM **1**, or 50 μM **2** and injected into the lateral tail vein of mice. After 10 days, the mice were sacrificed, and their lungs were analyzed for surface tumor foci. *d*, counting the number of tumor foci showed a strong inhibition of experimental lung metastasis by **1** (*open squares*) and **2** (*open circles*) when compared with DMSO (*filled squares*) (n = 5–7).

lation and sialylation should not occur, since the relevant transferases require Galβ1–4GlcNAc-R core as a substrate (9). As predicted, treating U937 cells with **2** in the presence of [^{3}H]galactose and [^{3}H]fucose did not yield any radiolabeled oligosaccharides generated on the glycoside (Fig. 6, *b* and *d*), whereas multiple neutral and charged (sialylated and sulfated) oligosaccharides were assembled on **1** (Fig. 6, *a* and *c*) (7, 9). The lack of any glycosylated products was confirmed in nonradioactive experiments using mass spectrometry (data not shown). Since the parent compound **1** has been previously shown to inhibit sLe^X expression in U937 cells by preventing fucosylation of endogenous glycoprotein substrates (9), these new findings suggest that analog **2** inhibits the formation of sLe^X by a different mechanism.

Inspection of the crystal structure of β4Gal-T1 suggested that other C-4′ derivatives might have potent inhibitory activity by affecting its interaction with Asp-314, which hydrogen-bonds with the C-4′ hydroxyl group of the GlcNAc acceptor moiety. To this end, we synthesized a series of peracetylated analogs in which the C-3′ and C-4′ hydroxyl groups of the GlcNAc moiety were replaced by -H, -F, -N_3, -NH_2, or -OCH_3. Incubation of U937 cells with each peracetylated disaccharide revealed that all of the analogs diminished cell surface sLe^X expression in a dose-dependent manner and to a similar extent as **1** (Fig. 4).

Analog 2 Inhibits Experimental Tumor Metastasis—Since sLe^X expression on tumor cells correlates with poor prognosis and aggressive metastasis (1), inhibitors of sLe^X expression could have therapeutic value. Disaccharide **1** was previously shown to prevent experimental and spontaneous metastasis of murine LLC cells in mice due to inhibition of sLe^X expression and diminished binding of tumor cells with platelets (12, 13). Neither **1** nor **2** was toxic to LLC cells up to 50 μM based on trypan blue exclusion and growth rates (Fig. 7*a*). Both compounds **1** and **2** decreased binding of monoclonal antibody CSLEX-1 to LLC cells by 49 and 30%, respectively (Fig. 7*b*). Treatment of LLC cells with analog **2** also dramatically reduced lung-metastatic tumor formation (77 $\pm$ 12 tumors (n = 5) to 13 $\pm$ 6 (n = 5) in an experimental metastasis model using compound-treated *versus* vehicle (DMSO)-treated cells; $p < 0.001$) (Fig. 7, *c* and *d*). Some animals receiving compound-treated cells had only one or two tumor nodules in the lung (Fig. 7*d*). Treatment of cells with compound **1** yielded similar results, indicating that the antimetastatic activity of these compounds is related to their ability to bind galactosyltransferase(s) and either act as a primer (compound **1**) or as a competitive inhibitor (compound **2**).

In summary, analogs of GlcNAcβ1–3Galβ-*O*-NM block sLe^X expression presumably by competitively inhibiting the action of β4Gal-T1 or related galactosyltransferases. In contrast, the parent compound **1** inhibits cell surface sLe^X expression by a mechanism that involves priming of oligosaccharides and diversion of downstream enzymes involved in sLe^X biosynthesis on tumor cells, such as α2–3sialyltransferases and α1–4-

fucosyltransferase (9). The deacetylated form of the 4′-deoxy analog can bind to β4Gal-T1 *in vitro*, and assuming that this is the primary target *in vivo*, binding leads to effective inhibition of the enzyme for natural glycoprotein substrates. We presume that the deacetylated form of compound **2** is responsible for inhibition, but formally we cannot exclude the possibility that a partially deacetylated derivative also might have activity.

Further studies are needed to determine if β4Gal-T1 is the primary target or if other galactosyltransferase might be inhibited (23). Regardless, **2** and other analogs listed in Fig. 1 provide more selective agents for blocking cell surface sLe^X expression than inhibitors that act earlier in the pathway, such as *N*-acetylgalactosaminides, which block the formation of all *O*-GalNAc-linked glycans. Our finding that the IC_{50} value of **2** *in vivo* is ~5-fold less than the K_i value *in vitro* of the deacetylated compound for β4Gal-T1 indicates that if this enzyme is indeed the target, partial inhibition may suffice to block multivalent interactions between selectins and tumor cell glycoconjugates involved in cell adhesion. These data suggest that nonsubstrate disaccharides have therapeutic potential through their ability to alter glycan-dependent pathologic processes. Further studies are warranted to explore whether other types of disaccharides and their derivatives can act in a similar manner in other glycosylation pathways.

Acknowledgments—We thank Dr. Mark Fuster for helpful discussions, Dr. Alexander Wlodawer and Mi Li for help in data collection, and Najma Khorrami for help with crystallization.

REFERENCES

1. Witz, I. P. (2008) *Cancer Metastasis Rev.* **27,** 19–30
2. Chhabra, S. R., Rahim, A. S., and Kellam, B. (2003) *Mini Rev. Med. Chem.* **3,** 679–687
3. Barthel, S. R., Gavino, J. D., Descheny, L., and Dimitroff, C. J. (2007) *Expert Opin. Ther. Targets* **11,** 1473–1491
4. Brown, J. R., Fuster, M. M., and Esko, J. D. (2003) *Carbohydrate Based Drug Discovery* (Wong, C.-H. ed) pp. 883–898, Wiley VCH, Weinheim, Germany
5. Brown, J. R., Crawford, B. E., and Esko, J. D. (2007) *Crit. Rev. Biochem. Mol. Biol.* **42,** 481–515
6. Sarkar, A. K., Fritz, T. A., Taylor, W. H., and Esko, J. D. (1995) *Proc. Natl. Acad. Sci. U. S. A.* **92,** 3323–3327
7. Sarkar, A. K., Rostand, K. S., Jain, R. K., Matta, K. L., and Esko, J. D. (1997) *J. Biol. Chem.* **272,** 25608–25616
8. Sarkar, A. K., Brown, J. R., and Esko, J. D. (2000) *Carbohydr. Res.* **329,** 287–300
9. Brown, J. R., Fuster, M., Whisenant, T., and Esko, J. D. (2003) *J. Biol. Chem.* **278,** 23352–23359
10. Kojima, N., Handa, K., Newman, W., and Hakomori, S. (1992) *Biochem. Biophys. Res. Commun.* **182,** 1288–1295
11. Huang, J., Byrd, J. C., Yoon, W. H., and Kim, Y. S. (1992) *Oncol. Res.* **4,** 507–515
12. Fuster, M. M., Brown, J. R., Wang, L., and Esko, J. D. (2003) *Cancer Res.* **63,** 2775–2781
13. Brown, J. R., Fuster, M. M., Li, R., Varki, N., Glass, C. A., and Esko, J. D. (2006) *Clin. Cancer Res.* **12,** 2894–2901
14. Brockhausen, I., Benn, M., Bhat, S., Marone, S., Riley, J. G., Montoya-Peleaz, P., Vlahakis, J. Z., Paulsen, H., Schutzbach, J. S., and Szarek, W. A. (2006) *Glycoconj. J.* **23,** 525–541
15. Ramasamy, V., Ramakrishnan, B., Boeggeman, E., Ratner, D. M., Seeberger, P. H., and Qasba, P. K. (2005) *J. Mol. Biol.* **353,** 53–67
16. Brunger, A. T., Adams, P. D., Clore, G. M., DeLano, W. L., Gros, P., Grosse-Kunstleve, R. W., Jiang, J. S., Kuszewski, J., Nilges, M., Pannu, N. S., Read, R. J., Rice, L. M., Simonson, T., and Warren, G. L. (1998) *Acta Crystallogr. Sect. D Biol. Crystallogr.* **54,** 905–921
17. Jones, T. A., Zou, J. Y., Cowan, S. W., and Kjeldgaard, M. (1991) *Acta Crystallogr. Sect. A* **47,** 110–119
18. DeLano, W. L. T. (2002) *The PyMOL Molecular Graphics System*, DeLano Scientific, San Carlos, CA
19. Esko, J. D., Weinke, J. L., Taylor, W. H., Ekborg, G., Rodén, L., Anantharamaiah, G., and Gawish, A. (1987) *J. Biol. Chem.* **262,** 12189–12195
20. Morton, C. L., Wierdl, M., Oliver, L., Ma, M. K., Danks, M. K., Stewart, C. F., Eiseman, J. L., and Potter, P. M. (2000) *Cancer Res.* **60,** 4206–4210
21. Soares, E. R. (1979) *Biochem. Genet.* **17,** 577–583
22. Kavarana, M. J., Kovaleva, E. G., Creighton, D. J., Wollman, M. B., and Eiseman, J. L. (1999) *J. Med. Chem.* **42,** 221–228
23. Hennet, T. (2002) *Cell Mol. Life Sci.* **59,** 1081–1095
24. Asano, M., Nakae, S., Kotani, N., Shirafuji, N., Nambu, A., Hashimoto, N., Kawashima, H., Hirose, M., Miyasaka, M., Takasaki, S., and Iwakura, Y. (2003) *Blood* **102,** 1678–1685
25. Gastinel, L. N., Cambillau, C., and Bourne, Y. (1999) *EMBO J.* **18,** 3546–3557
26. Ramakrishnan, B., and Qasba, P. K. (2001) *J. Mol. Biol.* **310,** 205–218
27. Ramakrishnan, B., Balaji, P. V., and Qasba, P. K. (2002) *J. Mol. Biol.* **318,** 491–502
28. Ramakrishnan, B., Boeggeman, E., and Qasba, P. K. (2004) *Biochemistry* **43,** 12513–12522
29. Ramakrishnan, B., Ramasamy, V., and Qasba, P. K. (2006) *J. Mol. Biol.* **357,** 1619–1633
30. Sinha, S. K., and Brew, K. (1980) *Carbohydr. Res.* **81,** 239–247
31. Hindsgaul, O., Kaur, K. J., Srivastava, G., Blaszczyk-Thurin, M., Crawley, S. C., Heerze, L. D., and Palcic, M. M. (1991) *J. Biol. Chem.* **266,** 17858–17862
32. Wong, C.-H., Ichikawa, Y., Krach, T., Gautheron-Le Narvor, C., Dumas, D. P., and Look, G. C. (1991) *J. Am. Chem. Soc.* **113,** 8137–8145
33. Kajihara, Y., Hashimoto, H., and Kodama, H. (1992) *Carbohydr. Res.* **229,** C5–C9
34. Chung, S. J., Takayama, S., and Wong, C. H. (1998) *Bioorg Med. Chem. Lett.* **8,** 3359–3364
35. Kajihara, Y., Kodama, H., Endo, T., and Hashimoto, H. (1998) *Carbohydr. Res.* **306,** 361–378
36. Saotome, C., Kanie, Y., Kanie, O., and Wong, C. H. (2000) *Bioorg. Med. Chem.* **8,** 2249–2261